[Journal of the Faculty of Science, Hokkaidô University, Japan, Ser. II, Vol. V, No. 5, 1961]

Nonstatic Effects in Proton-Proton Scattering below 150 Mev†

Ryozo TAMAGAKI, Wataro WATARI††
and Shoichiro OTSUKI†††

(Received Oct. 30, 1961)

Abstract

By analysing p–p scattering below 150 Mev, it is investigated p–p scattering data demand modifications of phase shifts given by the static pion-theoretical potentials. The purpose of this paper is not to find the best fit solution but to find main features of indispensable modifications to the static potentials. Analysis at 150 Mev shows spin-orbit coupling effect. To make clear its property, complete experiment at intermediate energies, especially measurement of C_{KP}, is important.

§ 1. Introduction

The static pion theory has succeeded to explain most of two-nucleon phenomena at low ($E \lesssim 20$ Mev) and intermediate ($E=20\sim100$ Mev) energies, E being the laboratory energy.[1] This success following the Taketani theory[2] is essentially owing to the properties of the tail of OPEP (one-pion-exchange potential), the most reliable part of the pion theory of nuclear forces. On the other hand, the p–p scattering experiments at 310 Mev have revealed the spin-orbit coupling effect at high energies.[3] The above two facts show the importance of analysing the p–p data at an energy around 100~150 Mev. At this energy reion, OPEP and TPEP (two-pion-exchange potential) in the regions I and II* play main roles, but inner interactions in the region III* have also appreciable effects if they are strong. Therefore, this energy region is appropriate to find modifications to be added to the static pion-theoretical potentials. Analysis is first made at 150 Mev and the connection to lower and higher energy data is discussed later.

HOSHIZAKI and MACHIDA[4] have shown that two-nucleon interations can be described by a local potential in good approximation, even though recoil effects

† Short report of this paper has been published in Genshikakukenkyu (in Japanese) Vol. 5, No. 1 (1960), 150 and 172.

†† Research Institute for Atomic Energy, Osaka City University, Osaka.

††† Institute for Theoretical Physics, Nagoya University, Nagoya.

* I is the region ($x \gtrsim 1.5$), II the region ($0.7 \lesssim x \lesssim 1.5$) and III the region ($x \lesssim 0.7$), where x is the internucleon distance in unit of the pion-Compton wave length $\hbar/\mu c$, μ being the pion mass.

are fully taken into account. It is adequate to discuss behaviors of phase shifts with an assumption that they are yielded by a local potential, which has the following form:

$$V(x)=V_C+V_TS_{12}+V_{LS}\boldsymbol{L}\cdot\boldsymbol{S}+V_{LL}(\sigma_1\boldsymbol{L})(\sigma_2\cdot\boldsymbol{L})+V'_{LL}\boldsymbol{L}^2+V_p \quad (1)$$

where V_C etc depend on the total spin S and parity Π (denoted as ${}^{2S+1}V_C^{\Pi}$ etc). Static potentials contain the first two terms. The other terms are non-static ones. V_p means the explicitly momentum-dependent term, which appears together with V_{LL} and V'_{LL} terms.

These last three terms are small by one order of magnitude compared with V_C, V_T and V_{LS}. However, we retain V_{LL} and V'_{LL} because of their large kinematical factors for high L values, but we neglect V_p.

For convenience sake the kinematical factors of the potential (1) are explicitely written down in Table 1. The relation,

$$(\sigma_1\cdot\boldsymbol{L})(\sigma_2\cdot\boldsymbol{L})\equiv\frac{1}{2}\left\{(\sigma_1\cdot\boldsymbol{L})(\sigma_2\cdot\boldsymbol{L})+(\sigma_2\cdot\boldsymbol{L})(\sigma_1\cdot\boldsymbol{L})\right\}=(\boldsymbol{L}\cdot\boldsymbol{S})^2-\delta_{L,J}L(L+1),$$

is used. The same notations with ref. 1a) are used.

Such an approach as attempted in this paper has been previously made in analysing angular distribution $I_0(\theta)$ and polarization $P(\theta)$ in p–p and n–p scattering at 150 Mev by one of anthors (*R. T.*).[1d] As far as we concerned $I_0(\theta)$ and $P(\theta)$, we did not find positive evidence for nonstatic effects (the solution obatined corresponds to the case i here). In this paper, we extend analysis to triple scattering and spin correlation parameters recently measured in p–p scattering.

§ 2. Phase shifts at 150 Mev

Below about 100 Mev, the static part of OPEP is known to play a main role in the angular distribution $I_0(\theta)$ and the polarization $P(\theta)$, and the connection of the potential features and the data has been investigated in detail. The potenital with the OPEP-tail can reproduce $I_0(\theta)$ and $P(\theta)$ below 100 Mev, which is denoted as SPOT (static potential with OPEP-tail)[1f]:

$${}^3V^-_{\rm SPOT}={}^3V^-_C+{}^3V^-_TS_{12}$$

$$=\begin{cases}\mu c^2(g^2/4\pi)(1/3)\{1+S_{12}(1+3/x+3/x^2)\}e^{-x}/x & \\ \text{with}\quad g^2/4\pi=0.08 & (x>1.0),\\ V_C(\mathrm{II})+V_T(\mathrm{II})S_{12}=(-20+10S_{12})\,\mathrm{Mev} & (1.0\geq x>0.7),\\ V_C(\mathrm{III})+V_T(\mathrm{III})S_{12}=-100\,\mathrm{Mev} & (0.7\geq x>0.32),\\ +\infty & (x\leq {}^3x^-_C=0.32).\end{cases} \quad (2)$$

TABLE 1. Potential of Eq. (1) in each two-nucleon state. T is the total isotopic spin. Only the $T=1$ state concerns with p-p scattering. The coupling terms due to tensor potentials are shown by $*$.

$T=1$

J	$S=0,\ \Pi=+1$		$S=1,\ \Pi=-1$	
0	$^1S_0$	V_C	$^3P_0$	$V_C-4V_T \quad -2V_{LS}+4V_{LL}+2V'_{LL}$
1			$^3P_1$	$V_C+2V_T \quad -V_{LS}-V_{LL}+2V'_{LL}$
2	$^1D_2$	$V_C-6V_{LL}+6V'_{LL}$	$^3P_2$	$V_C-(2/5)V_T+(6\sqrt{6}/5)V_T^* \quad +V_{LS}+V_{LL}+2V'_{LL}$
			$^3F_2$	$V_C-(8/5)V_T+(6\sqrt{6}/5)V_T^* \quad -4V_{LS}+16V_{LL}+12V'_{LL}$
3			$^3F_3$	$V_C+2V_T \quad -V_{LS}-11V_{LL}+12V'_{LL}$
4	$^1G_4$	$V_C-20V_{LL}+20V'_{LL}$	$^3F_4$	$V_C-(2/3)V_T+(4\sqrt{5}/3)V_T^* \quad +3V_{LS}+9V_{LL}+12V'_{LL}$
			$^3H_4$	$V_C-(4/3)V_T+(4\sqrt{5}/3)V_T^* \quad -6V_{LS}+36V_{LL}+30V'_{LL}$
5			$^3H_5$	$V_C+2V_T \quad -V_{LS}-29V_{LL}+30V'_{LL}$
6	$^1I_6$	$V_C-42V_{LL}+42V'_{LL}$	$^3H_6$	$V_C-(10/13)V_T+(6\sqrt{42}/13)V_T^* \quad +5V_{LS}+25V_{LL}+30V'_{LL}$

$T=0$

J	$S=0,\ \Pi=-1$		$S=1,\ \Pi=+1$	
1	$^1P_1$	$V_C-2V_{LL}+2V'_{LL}$	$^3S_1$	$V_C \quad +\sqrt{8}V_T^*$
			$^3D_1$	$V_C \quad -2V_T \quad +\sqrt{8}V_T^* \quad -3V_{LS}+9V_{LL}+6V'_{LL}$
2			$^3D_2$	$V_C+2V_T \quad -V_{LS}-5V_{LL}+6V'_{LL}$
3	$^1F_3$	$V_C-12V_{LL}+12V'_{LL}$	$^3D_3$	$V_C-(4/7)V_T+(12\sqrt{3}/7)V_T^* \quad +2V_{LS}+4V_{LL}+6V'_{LL}$
			$^3G_3$	$V_C-(10/7)V_T+(12\sqrt{3}/7)V_T^* \quad -5V_{LS}+25V_{LL}+20V'_{LL}$
4			$^3G_4$	$V_C+2V_T \quad -V_{LS}-19V_{LL}+20V'_{LL}$
5	$^1H_5$	$V_C-30V_{LL}+30V'_{LL}$	$^3G_5$	$V_C-(8/11)V_T+(6\sqrt{30}/11)V_T^* \quad +4V_{LS}+16V_{LL}+20V'_{LL}$
			$^3I_5$	$V_C-(14/11)V_T+(6\sqrt{30}/11)V_T^* \quad -7V_{LS}+49V_{LL}+42V'_{LL}$
6			$^3J_6$	$V_C+2V_T \quad -V_{LS}-41V_{LL}+42V'_{LL}$

Above 100 Mev, this case is taken on trial, and non-static terms are added to it. The triplet odd phase shifts* at 150 Mev given by the potential Eq. (2) are:

$$\begin{aligned} J=0\ ;&\quad {}^3\delta_0=0.568\\ 1\ ;&\quad {}^3\delta_1=-0.170\\ 2\ ;&\quad {}^3\delta_2^{\alpha}=0.176,\quad \varepsilon_2=-0.432,\quad {}^3\delta_2^{\gamma}=-0.010\\ 3\ ;&\quad {}^3\delta_3=-0.046\\ 4\ ;&\quad {}^3\delta_4^{\alpha}=0.023,\quad {}^3\delta_4^{\gamma}=-0.010,\quad \varepsilon_4=-0.690\\ 5\ ;&\quad {}^3\delta_5=-0.010, \end{aligned} \tag{3}$$

which are characterized by

$$ {}^3\delta_0 \gg {}^3\delta_2^{\alpha} > 0 > {}^3\delta_1 \quad \text{and} \quad 0 \gg \varepsilon_2 , \tag{4}$$

mainly because ${}^3V_T > 0$. Then necessary modifications are following.

(A) $P(\theta)$

$P(\theta)$ is decomposed as**

$$P(\theta) = (4\sin\theta/I_0k^2)\sum_{n=\text{odd}} a_n P_n(\cos\theta) , \tag{5}$$

where the main term a_1 is due to the interference between ${}^3P_J$-waves, i.e.,

$$a_1 \simeq a_1(P) \equiv (3/2) f(\varepsilon_2) \left\{ [{}^3\delta_0 | {}^3\delta_2^{\alpha}] + (3/2)[{}^3\delta_1 | {}^3\delta_2^{\alpha}] \right\} ,$$

where

$$[\delta_A | \delta_B] = \sin\delta_A \sin\delta_B \sin(\delta_A - \delta_B)$$

and

$$f(\varepsilon_2) = \cos 2\varepsilon_2 + (1/2\sqrt{6})\sin 2\varepsilon_2 .$$

Experimental data near 150 Mev ($P(45°) \simeq 0.22$) restrict a_1 as

$$a_1(\text{exp}) = 0.08 \sim 0.10.$$

The potential SPOT gives $a_1 = 0.047 \sim (1/2) a_1(\text{exp})$, where $a_1(P) = 0.038$. To make a_1 larger, a potential attractive in the ${}^3P_2$ state should be added, which increases ${}^3\delta_2^{\alpha}$ and $f(\varepsilon_2)$. The correlation between ${}^3\delta_2^{\alpha}$ and ε_2 is shown in Fig. 1 (qualitatively has been already discussed in ref. 1e)). As choice of such an attractive potential there are five possible ways and their combinations:

i) attractive central,
ii) positive tensor,
iii) negative spin-orbit,

* We use the nuclear BLATT-BIEDENHARN's phase shifts in radians throughout this paper.
** For detailed formula, see ref. 1d).

iv) negative quadratic spin-orbit coulping,
v) negative quadratic orbit-coupling.

Case i) Addition of ${}^3V_C^- < 0$. All e ${}^3P_J$-phase shifts increase. Such a case s already been investigated in ref. 1e). or example, SPOT with the smaller core sius ${}^3x_C^- = 0.28$, which is equivalent to addition of attractive potentials repro- ces the data of $I_0(\theta)$ and $P(\theta)$, if the iglet even phase shifts are properly osen.[1e] The resulting phase shifts are follows:

$$\left.\begin{aligned} &\text{plet odd};\ {}^3\delta_0 = 0.63,\ {}^3\delta_1 = -0.14,\\ &\qquad {}^3\delta_2^\alpha = 0.21,\ \ \varepsilon_2 = -0.35,\\ &\text{iglet even};\ {}^1\delta_0 = -0.01,\ {}^1\delta_2 = 0.15. \end{aligned}\right\} \quad (6)$$

$_0|{}^3\delta_2^\alpha|$ term becomes the main one in (θ) and $a_1(P) = 0.062$.

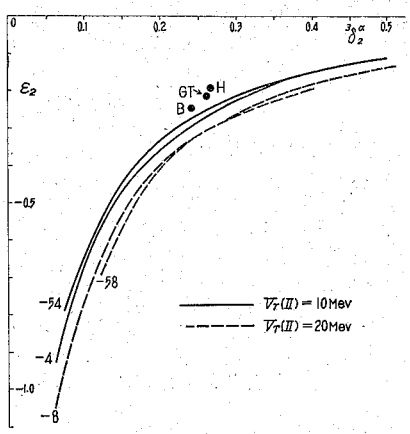

Fig. 1. Correlation between ${}^3\delta_2^\alpha$ and ε_2, obtained by various potentials of the type Eq. (2). Two cases of V_T(II) are plotted. The number attached to each curve is the potential depth (Mev) in the ${}^3P_2$-state except the ${}^3P_2$-coupling term. GT, B and GT are the same in Fig. 6.

Case ii) Addition of ${}^3V_T^- > 0$. The solute values of all ${}^3P_J$-wave phase shifts crease, then the effective total cross ction σ_t^{eff} becomes too large as discussed ref. 1e). So, this case is excluded.

Case iii) Addition of ${}^3V_{LS}^- < 0$. ${}^3\delta_0$ decreases, while $|{}^3\delta_1|$ and ${}^3\delta_2^\alpha$ increase, en the main term in a_1 becomes $(9/4)f(\varepsilon_2)[{}^3\delta_1|{}^3\delta_2^\alpha]$. To reproduce the data of (θ), $a_1(P) \sim 0.7$ with the estimated higher wave contribution, a_1 (higher wave) 0.15, consequently

$$\begin{aligned} &{}^3\delta_1 = -0.32 \sim -0.28,\\ &{}^3\delta_2^\alpha = 0.25 \sim 0.27 \ \text{ and } \ \varepsilon_2 = -0.25 \sim -0.20. \end{aligned} \quad (7)$$

In $\sigma_t^{eff} \equiv (1/2)\int d\Omega\,(1/k^2)\sum_l b_l^{(1)} P_l(\cos\theta)$, $\sigma_t^{eff}(\text{exp}) \cong 25$ mb implies $^{1)} = \sum_L (2L+1)(\sin {}^1\delta_L)^2 + \sum_{J,\rho=\alpha,\beta,\gamma}(2J+1)(\sin {}^3\delta_J^\rho)^2 \cong 0.73$ at 150 Mev. ibtracting the higher wave and the singlet even contributions (see qs. (3) and (9)), we get

$$(\sin {}^3\delta_0)^2 + 3(\sin {}^3\delta_1)^2 + 5(\sin {}^3\delta_2^\alpha)^2 \cong 0.58.$$

he substitution of the values of Eq. (7) leads to

$${}^3\delta_0 = 0 \sim 0.2, \quad (8)$$

if ${}^3\delta_0<0$ is discarded because of the continuity to the lower energy region. This reduction of ${}^3\delta_0$ is consistent with ${}^3V_{LS}^-<0$.

Case iv) Addition of ${}^3V_{LL}^-<0$. Its effects to ${}^3\delta_1$, ${}^3\delta_2^\alpha$ and ε_2 are same with ${}^3V_{LS}^-<0$. But the resulting condition ${}^3\delta_0=0\sim0.2$ is not satisfied, since ${}^3V_{LL}^-$ works an attractive force in the ${}^3P_0$ state contrary to ${}^3V_{LS}^-$.

Case v) Addition of ${}^3V_{LL}^1<0$. Its effects are same as in the case i.

(B) $R(\theta=90°)$

The data of R show $R(90°)\sim0$ (probably $|R(90°)|<0.1$) at 150 Mev. $R(90°)$ reflects the interference effects between the singlet even and the triplet odd potentials: In Stapp's notation[3a] $I_0R(90°)=(1/2)\mathrm{Re}(M_{01}^*M_{ss})\cong(1/2)\mathrm{Re}\,M_{01}\,\mathrm{Re}\,M_{ss}$.

Since M_{01} is independent of ${}^3\delta_0$, and $\mathrm{Re}\,M_{01}=-0.6\sim-0.8\times10^{-13}$ cm in the cases i)$\sim$iii), $R(90°)\sim0$ implies that

$$\mathrm{Re}\,M_{ss}=(1/k)\left\{\sin 2{}^1\delta_0-(5/2)\sin 2{}^1\delta_2+(27/8)\sin 2{}^1\delta_4\right\}\simeq0\,. \quad (9)$$

Neglecting the small ${}^1G_4$-contribution (${}^1\delta_4\sim0.01$), we obtain

$$\sin 2{}^1\delta_0\cong(5/2)\sin 2{}^1\delta_2\,.$$

Further, on the one hand, the low energy behavior of ${}^1\delta_0$ together with the MMS[3b] No. 1 solution at 310 Mev restricts ${}^1\delta_0$ as ${}^1\delta_0\lesssim0.3$. On the other hand, the OPEP-tail predicts ${}^1\delta_2=0.1\sim0.2$. From these informations, the singlet even phase shifts can be estimated as

$${}^1\delta_0=0.32\sim0.26 \quad \text{and} \quad {}^1\delta_2=0.10\sim0.12. \quad (10)$$

These values are consistent with the solution b at 210 Mev.[5]

If either ${}^1\delta_0$ decreases or ${}^1\delta_2$ increases or both from the values in Eq. (10), $\mathrm{Re}\,M_{ss}$ decreases, and $R(90°)$ becomes too large. The situation is shown in Fig. 2.

It is to be noted that the singlet even phase shifts given by Eq. (10) are different from those of Eq. (6) in the case i (and also in the case v). Thus the possibility i (and v) may not be real since the isotropy of $I_0(\theta)$ and $R(90°)\sim0$ are not compatible.

(C) Angular dependence of $R(\theta)$ near 90°

For the case i and iii the angular dependence of $R(\theta)$ are quite different. The case i (and v) is characterized by rapid decrease about 90° and the case iii by symmetry about 90°, as is shown in Fig. 2. This fact can be understood by calculating the conefficients of $(\cos\theta)^1$-term in the expansion of $R(\theta)$. According to Stapp's notation,

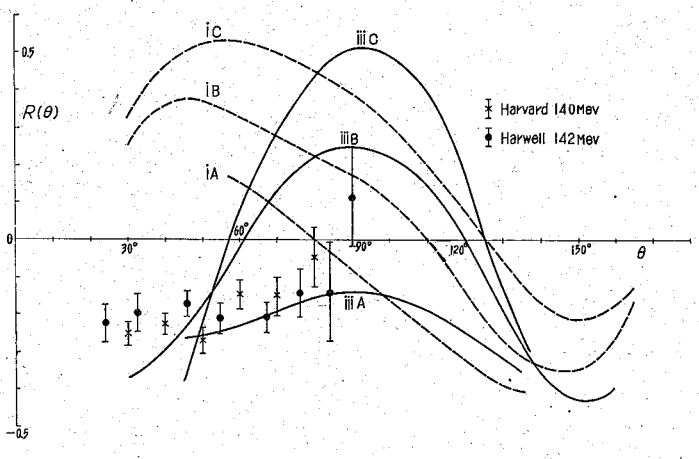

Fig. 2. $R(\theta)$ of p-p scattering at 150 Mev.
------ for case i; the ${}^3P_J$-phase shifts is given by Eq. (6).
—— for case iii; the ${}^3P_J$-phase shifts is given by Eq. (7) and ${}^3\delta_0=0.06$.
The singlet even phase shifts are
A: ${}^1\delta_0=0.30$, ${}^1\delta_2=0.10$, B: ${}^1\delta_0=0.21$, ${}^1\delta_2=0.15$, C: ${}^1\delta_0=-0.01$, ${}^1\delta_2=0.15$.

$$I_0R(\theta)=(1/2)\cos(\theta/2)\,\mathrm{Re}\left\{(M_{00}-\sqrt{2}\tan(\theta/2)M_{10})(M_{11}+M_{1-1}+M_{ss})^*\right.$$
$$\left.+(\sqrt{2}/\sin\theta)(M_{10}+M_{01})M_{ss}^*\right\},$$

where the real parts are main in all scattering matices. By noticing $\mathrm{Re}\,M_{ss}\simeq 0$ in Eq. (9) and retaining only the ${}^3P_J$-wave contribution in the $(\cos\theta)^1$ term, we obtain the approximate expression for I_0R near $\theta=90°$;

$$I_0R(\theta)\cong-(1/\sqrt{2})\sin(\theta/2)\,\mathrm{Re}\,M_{10}\,\mathrm{Re}(M_{11}+M_{1-1})$$
$$\cong(3/4k^2)\sin(\theta/2)\sin\theta\cos\theta\left\{\sin 2{}^3\delta_0-(\cos^2\varepsilon_2+\sqrt{3}\sin 2\varepsilon_2/2\sqrt{2})\sin 2{}^3\delta_2^\alpha\right\}$$
$$\times\left\{\sin 2{}^3\delta_1+(\cos^2\varepsilon_2-\sqrt{2/3}\sin 2\varepsilon_2)\sin 2{}^3\delta_2^\alpha\right\}.$$

nserting the values (6) and (7) for ${}^3\delta_2^\alpha$ and ε_2, we obtain

$$I_0R\cong(3/4k^2)\sin(\theta/2)\sin\theta\cos\theta\left(\sin 2{}^3\delta_0-\begin{cases}0.20\\0.31\sim0.37\end{cases}\right)\left(\sin 2{}^3\delta_1+\begin{cases}0.57\\0.64\sim0.66\end{cases}\right)$$
$$=(3/4k^2)\sin(\theta/2)\sin\theta\cos\theta\begin{cases}0.22 & \text{for the case i.}\\ -0.04\sim0.00 & \text{for the case iii.}\end{cases}$$

As the above equation shows, the value that

$$^3\delta_1\sim-0.3\quad\text{and/or}\quad{}^3\delta_0=0.1\sim0.15 \tag{10}$$

s sufficient to reproduce a small ciefficients of $(\cos\theta)^1$-term which the data

demand. Thus the experiments of R rule out the case i, and favour the case iii.

(D) $D(\theta)$

It is known that $D(\theta)$ at $\theta\sim 90°$ is sensitive to ${}^3\delta_0$.[14),16),1f)] Detailed discussions have already given in ref. 6). The sensitivity of $D(90°)$ to ${}^3\delta_0$ is shown in Fig. 3. Although $D(\theta)$ at $\theta\sim 90°$ has not yet been so definitely determined, ${}^3\delta_0$ is restricted as

$$ {}^3\delta_0 = 0\sim 0.2 \tag{11}$$

which is consistent with $I_0(\theta)$ and σ_t^{eff} (see Eq. (8)) in the case iii. Harvard and new Harwell data allow only the case iii.

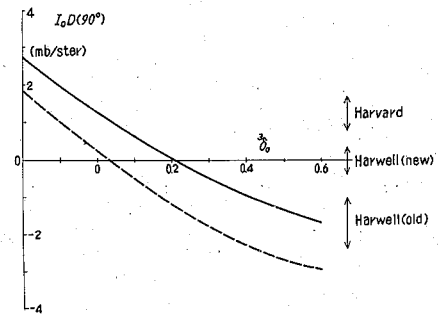

Fig. 3. Dependence of $I_0D(90°)$ on ${}^3\delta_0$ (the ${}^3P_0$ phase shift).
……; the triplet odd phase of SPOT given in Eq. (2).
——; ${}^3\delta_1=-0.30$, ${}^3\delta_2^{\alpha}=0.25$ and $\varepsilon_2=-0.21$ corresponding to the case iii and the other higher wave phase shifts in Eq. (3).

The resulting phase shifts compatible with the data at 150 Mev are:

$$\begin{aligned} &\text{singlet even;} \quad {}^1\delta_0 = 0.26\sim 0.32 \quad \text{and} \quad {}^1\delta_2 = 0.10\sim 0.12, \\ &\text{triplet odd;} \quad {}^3\delta_0 = 0\sim 0.2, \quad {}^3\delta_1 = -0.32\sim -0.28, \\ &\qquad\qquad {}^3\delta_2^{\alpha} = 0.25\sim 0.27 \quad \text{and} \quad \varepsilon_2 = -0.25\sim -0.20. \end{aligned} \tag{12}$$

The characteristic feature is ${}^3\delta_2^{\alpha} > {}^3\delta_0 > 0 \gg {}^3\delta_1$, which is the type yielded by ${}^3V_T^- > 0$ plus ${}^3V_{LS}^- < 0$. These values are consistent with the solutions of phase shift analysis recently made.[7)]

§ 3. Modification to static potentials

Comparing these values with those in (3) given by the static OPEP case, we find necessary modifications imposed on the static pion-theoretical potentials. This can be done most easily in correlation diagrams between the ${}^3P_J$-phase

hifts by considering the kinematical factors shown in Table 1.

From Fig. 4, some negative spin-orbit potentials should be added. The nost drastic change is seen in $^3\delta_0$, because the effect of $^3V_{\bar{LS}}<0$ to $^3\delta_0$ is re-)ulsive $(-2\,^3V_{\bar{LS}})$ and diminish the role of the OPEP positive tensor potential $-4\,^3V_T$), while in the $^3P_1$ and $^3P_2$ states the effects of ^3V_T and $^3V_{\bar{LS}}$ are in he same direction.

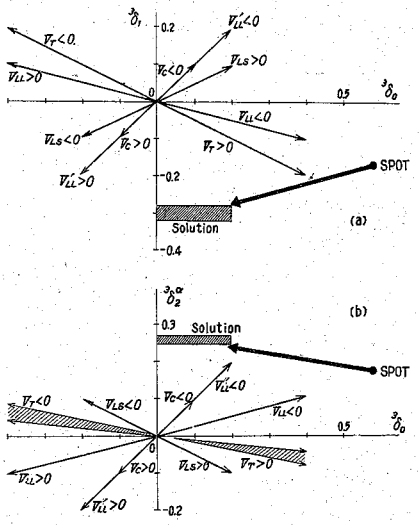

Fig. 4. Correlation between the ^3P_J-phase shifts. The arrows from the origin show the directions of modifications given by the kinematical factors of various potential terms in Table 1. (a) $^3P_0$-$^3P_1$ correlation; (b) $^3P_0$-$^3P_1$ correlation.

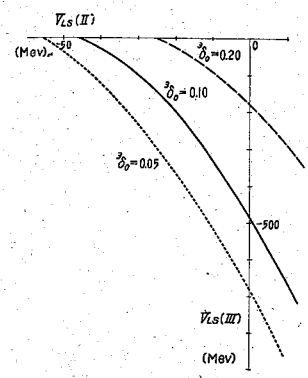

Fig. 5. Depth of $^3V_{\bar{LS}}$ in the region II and III necessary to reproduce good values of $^3\delta_0$ at 150 Mev. $V_C(\mathrm{II})=0$, $V_T(\mathrm{II})=10$ Mev, $V_C(\mathrm{III})=V_T(\mathrm{III})=0$ and $^3x_c=0.30$ are assumed.

Magnitude of necessary $^3V_{\bar{LS}}<0$ is estimated from $^3\delta_0$. In Fig. 5, the results calculated by the two-step-square well potential with the OPEP-tail are shown, where in the region II ($x=0.7\sim1.0$) $V_C(\mathrm{II})=0$, $V_T(\mathrm{II})=10$ Mev and in the region III ($x=0.3\sim0.7$) $V_C(\mathrm{III})=V_L(\mathrm{III})=0$ are assumed. We can estimate the strength of $^3V_{\bar{LS}}$: for example, by taking $V_{LS}(\mathrm{II})=-10$ Mev,

$$\begin{cases} {}^3\delta_0=0.20 & V_{LS}(\mathrm{III})\cong-100\ \mathrm{Mev} \\ {}^3\delta_0=0.10 & V_{LS}(\mathrm{III})\cong-300\ \mathrm{Mev} \\ {}^3\delta_0=0.05 & V_{LS}(\mathrm{III})\cong-500\ \mathrm{Mev}. \end{cases}$$

Weak cases correspond to Harwell data of D. Storng cases correspond to Harvard data of D and have the similar feature to GAMMEL and THALER's,[8]

SIGNELL and MARSHAK's,[9] BRYAN's[10] and HAMADA's[11] ${}^3\bar{V}_{LS}$. It should be emphasized that ${}^3\bar{V}_{LS}$ necessary at 150 Mev can be confined completely in the region III if we want. Therefore, we do not necessarily need the spin-orbit coupling potential, if the boundary condition at $x=0.7$ and the OPEP plus TPEP for $x>0.7$ are used. Such an approach has been successfully made.[12),13)]

For comparison, in Fig. 6, we plot the S, P and D phase shifts for SPOT (static potdntial with the OPEP-tail) and those for the potentials with the strong ${}^3\bar{V}_{LS}$[8)~11)]. The parameters of SPOT compatible with $I_0(\theta)$ and $P(\theta)$ below

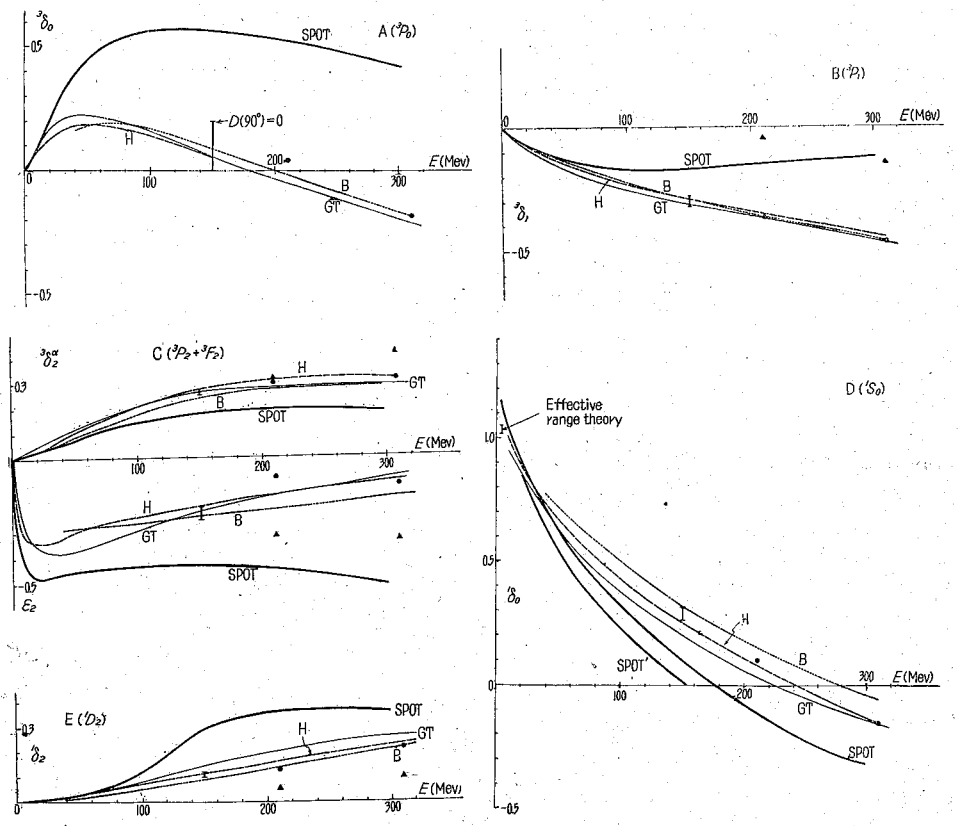

Fig. 6. Energy dependences of phase shifts ($L\leq 2$). SPOT shows the values due to the static potential, Eq. (2) and Eq. (13). SPOT′ in ${}^1\delta_0$ is the best fit to $I_0(\theta)$ below 150 Mev for the triplet odd potential Eq. (2). GT, B and H denote the values by GAMMEL-THALER's,[8] BRYAN's[10] and HAMADA's[11] potentials, respectively. I shows the values of Eq. (12) at 150 Mev.

● and ▲ at 310 Mev denote the solutions, MMS No. 1 and No. 2. Similarly ● and ▲ at 210 Mev denote the solutions, b and c, in ref. 5).

100 Mev are:

triplet odd; Eq. (2),

singlet even;[1e]
$$ {}^1V^+ = \begin{cases} \mu c^2(g^2/4\pi)e^{-x}/x \quad \text{with } g^2/4\pi=0.08 & (x>1.5), \\ -20 \text{ Mev} & (x=0.7\sim1.5), \\ -630 \text{ Mev} & (x=0.45\sim0.7), \\ +\infty & (x<{}^1x_C^+=0.45). \end{cases} \tag{13} $$

A remarkable difference is seen in ${}^3\delta_0$. Although differences in ${}^3\delta_1$, ${}^3\delta_2^\alpha$ and ε_2 seems to be small, due to the large kinematical factors related to them there appear large differences in some observed quantities. In the singlet even phase shifts there also exist the differences to compensate those of the triplet odd contributions to $I_0(\theta)$. In SPOT, rapid decrease in ${}^1\delta_0$ and rapid increase in ${}^1\delta_2$ above 100 Mev are characteristic. This feature is unfavorable for explanation of high energy data, as will been seen in the next section.

§ 4. Energy dependence of triple scattering and spin correlation paramaters

The spin-orbit coupling potentials necessary to reproduce the p–p scattering data near 150 Mev are strong. Therefore, even though their range is short, effects at lower energies will be appreciable (e.g. Fig. 6 shows a noticeable change of ${}^3\delta_0$ due to ${}^3V_{LS}^-$). At low ($E\lesssim20$ Mev) and intermediate ($E=20\sim100$ Mev) energies $I_0(\theta)$ and $P(\theta)$ are well reproduced by SPOT. By observing energy dependence of triple scattering and spin correlation parameters, we try to find suitable experiments to know further evidences on the nonstatic effects due to ${}^3V_{LS}^-$ at low and intermediate energies.

First we consider energy dependence of D, R, A, C_{nn} and C_{KP} at $\theta=90°$. We must to consider angular dependence if the values at $\theta=90°$ are insensitive to the nonstatic effects. Fig. 7 shows that $D(90°)$, $A(90°)$ and $C_{KP}(90°)$ are sensitive to the ${}^3V_{LS}^-$ effects. Especially C_{KP} is affected by ${}^3V_{LS}^-$ even at low energies.

This special sensitivity to ${}^3V_{LS}^-$ is closely connected with the ${}^3P_0$-state phase shift ${}^3\delta_0$. The nonvanishing scattering matrices $\theta=90°$ are $M_{ss}\equiv<S=0|M|S=0>$, $M_{01}\equiv<S=1,\ m_S=0|M|S=1,\ m_S=1>$ and $M_{10}\equiv<S=1,\ m_S=1|M|S=1,\ m_S=0>$. Only M_{10} contains ${}^3\delta_0$. The following expressions at $\theta=90°$;

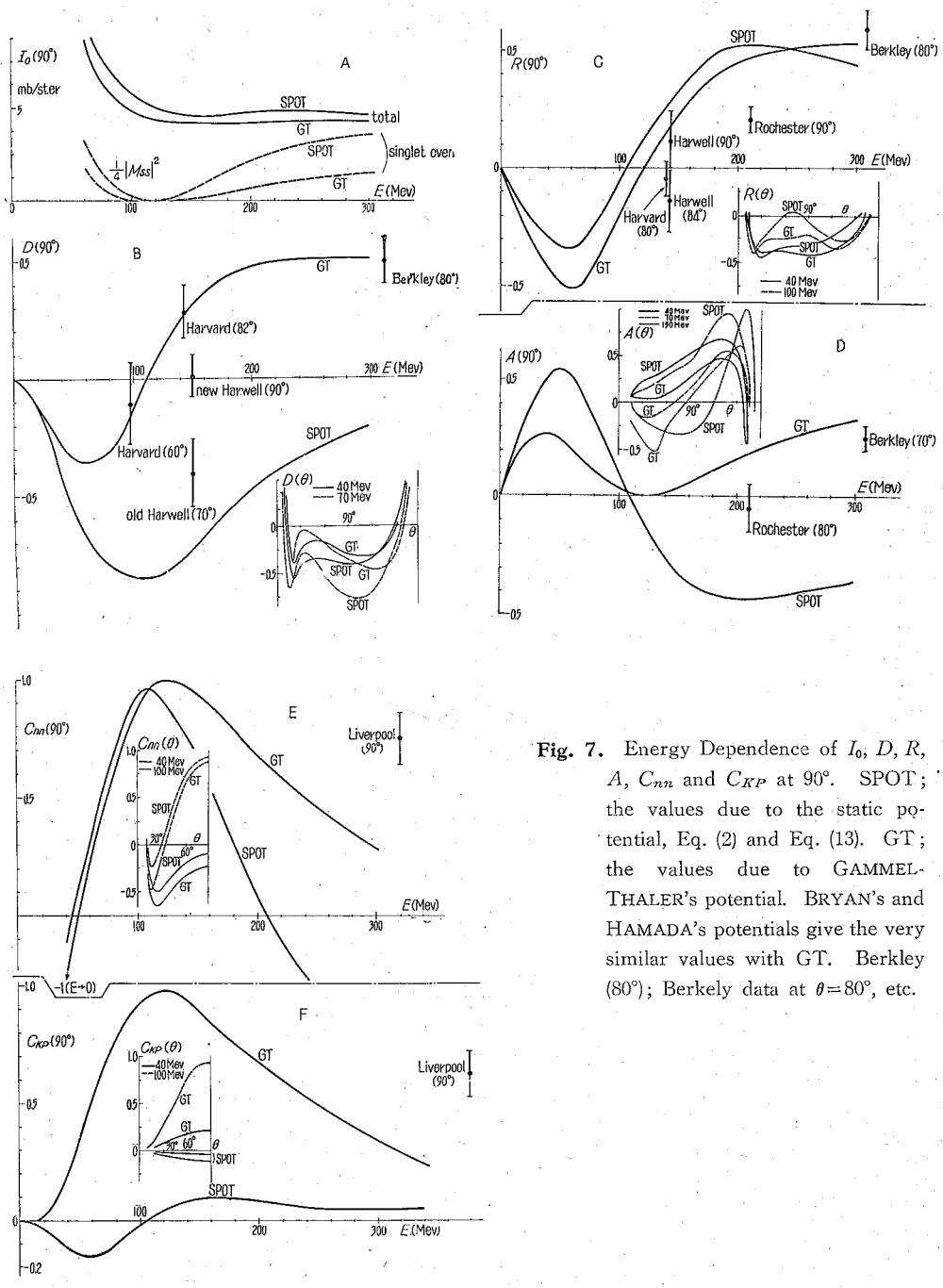

Fig. 7. Energy Dependence of I_0, D, R, A, C_{nn} and C_{KP} at 90°. SPOT; the values due to the static potential, Eq. (2) and Eq. (13). GT; the values due to GAMMEL-THALER's potential. BRYAN's and HAMADA's potentials give the very similar values with GT. Berkley (80°); Berkely data at $\theta=80°$, etc.

$$
\begin{aligned}
&I_0(90°)=(1/4)|M_{ss}|^2+(1/2)|M_{10}|^2+(1/2)|M_{01}|^2,\\
&I_0D(90°)=-(1/2)\mathrm{Re}(M_{10}M_{01}^*),\\
&I_0R(90°)=(1/2)\mathrm{Re}(M_{01}^*M_{ss}),\\
&I_0A(90°)=-(1/2)\mathrm{Re}(M_{10}^*M_{ss}),\\
&I_0C_{nn}(90°)=I_0(90°)-(1/2)|M_{ss}|^2=(1/2)|M_{01}|^2+(1/2)|M_{10}|^2-(1/4)|M_{ss}|^2,\\
&I_0C_{KP}(90°)=(1/2)(|M_{01}|^2-|M_{10}|^2),
\end{aligned}
\tag{14}
$$

show D, A and C_{KP} are dependent on M_{10}, and consequently on ${}^3\delta_0$.

Real parts are main in M_{ss}, M_{01} and M_{10}. They are shown in Fig. 8. By use of Eq. (14) and Fig. 8, we can understand characteristic features in Fig. 7.

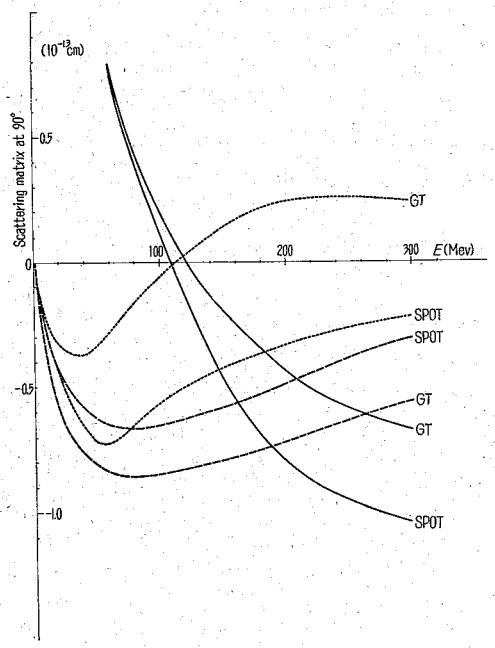

Fig. 8. Real parts of scattering matrices at $\theta=90°$, $\phi=0°$, ——; Mss, ----; M_{01} and ·····; M_{10}.
SPOT and GT mean the same in Fig. 7.

D. Deviation from SPOT is mainly due to the rapid decrease of ${}^3\delta_0$. The negative value of $D(90°)$ at $E\lesssim 100$ Mev results from the positive OPEP tensor part, and from type of the ${}^3P_J$-phase shifts in Eq. (4). The increase of the SPOT values for $E\gtrsim 100$ Mev comes from $1/k^2$-dependence of I_0D and $I_0\sim$ const..

R. The feature below 100 Mev is determined by OPEP ${}^3V_T>0$. The

sign-change at $E\sim 110$ Mev is due to that of Re M_{ss}. The data of Harvard, Harwell and Rochester demand the larger Re M_{ss} than SPOT and GT, which is one of evidences of smallness of ${}^1\delta_2$. The ${}^3V_{LS}^-$-effects reveal in the angular dependence of R(§2).

A. The positive $A(90°)$ $E\lesssim 100$ Mev is due to OPEP ${}^3V_T^->0$. The deviation from SPOT is the effect of ${}^3V_{LS}^-$ mainly through ${}^3\delta_0$. The sign change at $E\sim 110$ Mev comes from that of Re M_{ss} for SPOT, while $A(90°)$ for GT's and HAMADA's case remain positive at high energies because of the nearly simultaneous sign-change of Re M_{10}.

C_{KP}. Drastic deviation from SPOT can be understood as follows:

$$\text{SPOT};\quad |M_{01}|^2\sim|M_{10}|^2,\quad \text{then}\quad C_{KP}\sim 0,\quad \text{while}$$

$$\text{with strong}\quad {}^3V_{LS}^-<0;\quad |M_{01}|^2\gg|M_{10}|^2,\quad \text{then}\quad C_{KP}\gg 0.$$

Angular dependence is peaked at $\theta=90°$. Therefore, experiments of C_{KP} at $E=20\sim 200$ Mev are important. Especially experiments at $E\sim 50$ Mev provide useful informations to the ${}^3V_{LS}^-$ effect at low energies, as discussed in ref. 6). The large values of $C_{KP}(90°)\cong 1$ at $E\simeq 110$ Mev for GT's and HAMADA's case mean that the singlet contribution is small and $(1/2)|M_{01}|^2$ is the main part of $I_0(\theta)$.

C_{nn}. C_{nn} reflects differences of the singlet even contributions directly, even though I_0 is same. $C_{nn}(90°)<0(>0)$ at $E\lesssim 50$ Mev ($\gtrsim 50$ Mev) shows that the singlet contribution to I_0 is larger (smaller) than the triplet one. $C_{nn}(90°)\sim 1$ at $E\sim 120$ Mev is due to Re $M_{ss}=0$. The rapid decrease of C_{nn} at high energy side comes from that of Re M_{ss}. The data rule out such a rapid increase of ${}^1\delta_2$ as in SPOT and GT's and such a rapid decrease of ${}^1\delta_0$ as in SPOT. Measurements of $C_{nn}(90°)$ at $E\sim 50$ Mev provide a useful measure of ${}^1\delta_0$, since at these energies predictions of the effective range theory are not reliable but still the singlet higher wave contributions are yet small.

§ 5. Concluding Remarks

Modifications of the spin-orbit coupling type should be imposed on the static pion-theoretical potentials in the triplet odd state at 150 Mev. Origin of spin-orbit coupling interaction is an open question, since ${}^3V_{LS}^-$ of TPEP is too small to reproduce the data, even though recoil effects are fully taken into account. To seek for origin of this interaction experiments (especially C_{KP}) at low and intermediate energies are strongly wanted, because a range of ${}^3V_{LS}^-$ closely related to origin is made clear more directly at these energies than at high energies.

We know no positive evidence for the spin-orbit coupling potential in the riplet even state, while there is no strong objection for it, especially ${}^3V_{LS}^+>0$. Therefore, it is important to find n–p experiments from which we can say omething definite to ${}^3V_{LS}^+$.

This work has been done as a part of the 1960–61 Annual Research Project on the Theory of Nuclear Forces organized by the Research Institute for Fundamental Phisics, Kyoto University. The authors express their sincer thanks to Prof. M. TAKATANI, Dr. S. MACHIDA and Dr. N. HOSHIZAKI for thier valuable discussions. We are also indebted to Dr. T. HAMADA for his numerical calculations of phase shifts and scattering parameters by the static pion-theoretical potentials with OPEP-tail.

References

1) (a) IWADARE, OTSUKI, TAMAGAKI and WATARI: Supplement of Prog. Theor. Phys. No. 3 (1956), 32. (b) S. OTSUKI: Prog. Theor. Phys. **20** (1958), 171. (c) W. WATARI: Prog. Theor. Phys. **20** (1958), 181. (d) R. TAMAGAKI: Prog. Theor. Phys. **20** (1958), 505. (e) HAMADA, IWADARE, OTSUKI, TAMAGAKI and WATARI: Prog. Theor. Phys. **22** (1959), 566 and (f) **23** (1960), 366.
2) M. TAKETANI, S. NAKAMURA and M. SASAKI: Prog. Theor. Phys. **6** (1951), 581.
3) (a) H. P. STAPP, T. J. YPSILANTIS and N. METROPOLIS: Phys. Rev. **105** (1957), 302. (b) M. H. MACGREGOR, M. J. MORAVCSIK and H. P. STAPP: Phys. Rev. **116** (1959), 1248.
4) N. HOSHIZAKI and S. MACHIDA: Prog. Theor. Phys. **24** (1960), 1325 and ibid. (to be published).
5) M. H. MACGREGOR and M. J. MORAVCSIK: Phys. Rev. Lett. **4** (1960), 524.
6) S. OTSUKI, R. TAMAGAKI and W. WATARI: Prog. Theor. Phys. (to be published).
7) BREIT, HULL, LASSILA and PYATT: Phys. Rev. **120** (1960), 2227.
8) J. L. GAMMEL and R. M. THALER: Phys Rev. **107** (1957), 291.
9) P. S. SIGNELL and R. E. MARSHAK: Phys. Rev. **109** (1958), 1229.
10) R. A. BRYAN: Nouv. Cim. **16** (1960), 895.
11) T. HAMADA: Prog. Theor. Phys. **24** (1960), 220; **24** (1960), 1033.
12) D. P. SAYLORR, A. BRYAN and R. E. MARSHAK: Phys. Rev. Lett. **5** (1960). 266.
13) H. FESHBACH, E. LOMON and A. TUBIS: Phys. Rev. Lett. **6** (1961), 635.
14) B. P. NIGAM: Prog. Theor. Phys. **23** (1960), 61.